Wavelength Halving in a Transition between Standing Waves and Traveling Waves

Akiko Kaminaga, Vladimir K. Vanag, and Irving R. Epstein

Department of Chemistry and Volen Center for Complex Systems, MS 015, Brandeis University, Waltham, Massachusetts 02454, USA

(Received 30 March 2005; published 29 July 2005)

In the Belousov-Zhabotinsky reaction-diffusion system dispersed in a newly developed water-in-oil aerosol OT/Span-20 microemulsion, the transition between standing waves and traveling waves is accompanied by a halving of the wavelength.

DOI: 10.1103/PhysRevLett.95.058302 PACS numbers: 82.40.Ck, 02.70.Uu, 68.05.Gh, 82.33.Nq

The transition between standing waves (SW) and traveling waves (TW) is a well-known phenomenon in fluid convection [1,2] and in electrochemical dissolution [3]. In a number of experimental reaction-diffusion systems, standing waves, packet waves, and traveling waves arise as a result of a wave instability [4–9]. These transitions can be modeled using coupled complex Ginzburg-Landau equations [10,11] or reaction-diffusion equations [12,13]. In all cases studied to date, regardless of the nature of the medium, the wavelength remains unchanged during the transition between SW and TW.

In this Letter, we report the first experimental evidence for a SW-TW transition in which the wave number doubles. This phenomenon occurs in a newly developed reaction-diffusion system that resembles the Belousov-Zhabotinsky reaction dispersed in a water-in-oil aerosol OT [AOT is sodium bis(2-ethylhexyl) sulfosuccinate] microemulsion (BZ-AOT system) [8]. By replacing the octane used in that system with hexadecane and adding an additional nonionic surfactant, sorbitan monolaurate, Span-20 [14], we constructed a new BZ-microemulsion system (BZ-AOT/Span) that can be described by the molar ratios $\omega_2 = [H_2O]/([AOT] + [Span\text{-}20])$, $\rho = [Span\text{-}20]/[AOT]$ and the volume droplet fraction $\varphi_d = \varphi_s + \varphi_w$, where φ_s and φ_w are the total volume fraction of the two surfactants and the volume fraction of the aqueous pseudophase, respectively.

In order to understand the phenomena observed in this new microemulsion (ME), we need to understand its physical properties. We therefore performed a series of light scattering, electrical conductivity, and fast mixing experiments. Dynamic light scattering [see Figs. 1(a) and 1(b)] revealed that the ME consists of very large water droplets (or clusters of small water droplets), the hydrodynamic radius R of which increases with ρ and reaches 30–50 nm at $\rho = 0.4$–0.45. A further increase in ρ (above 0.5) leads to an opaque ME. Dilution of the ME with hexadecane (decreasing φ_d from 0.68 to 0.33) slightly decreased R (from 50 to 30 nm). Varying the temperature between 18 and 25 °C changed R by only about 10%, comparable to our experimental error. Figure 1(b) also demonstrates that R decreases with the concentration of electrolyte ($NaBrO_3$ or sulfuric acid).

Measurement of the electrical conductivity σ as a function of droplet fraction [Fig. 1(c)] shows that σ gradually increases with φ_d without the sharp percolation transition that occurs in pure AOT ME. At the droplet fractions used in our experiments ($\varphi_d = 0.5$–0.7), σ is close ($\sigma > 100\ \mu S/cm$) to the electrical conductivity of the pure aqueous phase, which suggests that the ME contains dynamical water channels. In this case the term "droplet" may not be a precise characterization of the aqueous pseudophase.

In the BZ-AOT system, there is, on average, less than one catalyst molecule per water droplet. Increasing R by an

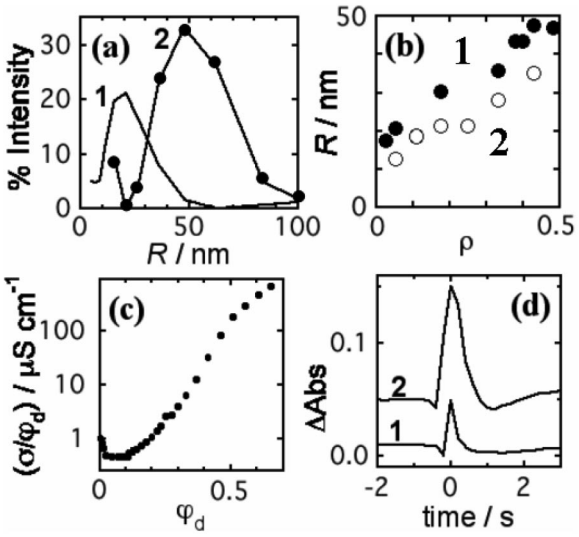

FIG. 1. Characteristics of AOT/Span ME at $\omega_2 = 11$. (a),(b) Light-scattering experiments with $\varphi_d = 0.66$: (a) distribution of radii of water droplets, R, loaded with composition 1 [MA (0.2 M), H_2SO_4 (0.22 M), and $NaBrO_3$ (0.3 M)], $\rho =$ (curve 1) 0.026, (curve 2) 0.429; (b) R vs ρ for ME loaded with (curve 1) composition 1, (curve 2) MA (0.4 M) and H_2SO_4 (0.44 M); (c) specific conductivity, σ/φ_d, of ME loaded with composition 1 and [bathoferroin] = 4 mM vs φ_d at $\rho = 0.429$; at $\varphi_d = 0$ (pure oil phase), $\sigma < 0.001\ \mu S/cm$; (d) kinetics of mass exchange obtained by fast mixing of two structurally identical MEs [$\rho = 0.429$, $\varphi_d =$ (1) 0.1 and (2) 0.3], one loaded with "acid" ([MA] = 0.22 M and $[H_2SO_4] = 0.24$ M), the other with bromcresol purple; mixing is stopped at time = 0.

order of magnitude in the BZ-AOT/Span system may lead to qualitative changes in behavior, since each water droplet now contains several hundred molecules of the catalyst (here, bathoferroin [15]) and tens of thousands of reactant molecules. Consequently, we may regard each droplet as a single nano-oscillator or nanoreactor.

The mass exchange rate, k_{ex}, which plays a key role in communication between nanoreactors, should be smaller for large droplets than for small droplets. To estimate the characteristic time of mass exchange for the BZ-AOT/Span system, we performed experiments in which a pair of MEs, one loaded with ''acid,'' the other with a pH indicator were rapidly mixed. We used a fast mixing cell from a stopped flow apparatus and introduced the two MEs through manually operated syringes. The resolution time of our homemade setup was 0.2 s. Experiments revealed that for $\varphi_d = 0.1$–0.3, the characteristic time of mass exchange due to collision or fusion or fission of droplets (or clusters) is less than our resolution time [Fig. 1(d)] and therefore significantly smaller than the characteristic times of the BZ kinetics (10–100 s).

Experiments on pattern formation were performed as in our earlier BZ-AOT studies [9,15]. Two stock MEs with the same ω_2, ρ, and φ_d were loaded, one (ME-1) with malonic acid (MA) and H_2SO_4, the other (ME-2) with bathoferroin and $NaBrO_3$. Equal volumes of ME-1 and ME-2 were mixed, and additional hexadecane was added if necessary to obtain the desired final φ_d. A small amount (0.16 mL) of the final reactive ME was sandwiched between two flat optical windows separated by an $h = 80$ μm thick annular Teflon gasket with inner and outer diameters 38 and 47 mm, respectively. The edges of this reactor sandwich were sealed with Teflon tape, and the windows were gently pressed together. The patterns were observed at ambient temperature (23–24 °C) through a microscope equipped with a CCD camera connected to a computer. Since we use hexadecane, which melts at about 18 °C, we first thermostatted the reactor but then found that there were no significant changes due to temperature in the range 20–25 °C. Simultaneously with our experiments on pattern formation, we observed the behavior of a BZ-AOT/Span system of the same composition in a well stirred tank reactor (STR), recording the absorption at 620 nm (arbitrary wavelength in the absorption band of the oxidized state of bathoferroin).

At some initial reactant concentrations with $\rho = 0.4$–0.45 and $\varphi_d = 0.6$–0.7, we observed a sharp transition from SW with wavelength λ_{SW} to TW with wavelength $\lambda_{TW} \cong \lambda_{SW}/2$ (Fig. 2). In a typical experiment, the first patterns observed are SW (for lower $[BrO_3^-] \approx 0.2$ M) or chaotic trigger waves (for $[BrO_3^-] \approx 0.3$ M) that transform over 15–40 min into the same SW seen at lower bromate concentrations [Figs. 2(a) and 2(b)]. The wavelength λ_{SW} increases slowly with time [Fig. 3(a), curve 1] and after 10–30 min, the SW transform into TW patterns [Fig. 2(d)]. For some initial reactant concentrations, this transition is very fast, like that shown in Fig. 2(e). For these cases $\lambda_{SW}/\lambda_{TW} = 2 \pm 0.2$. The error in determining the wavelength from the fast Fourier transform (FFT) is also about $\pm 10\%$. For other concentrations, the change occurs over 5–25 min [16] and $\lambda_{SW}/\lambda_{TW} = 1.4$–$2.0$. The rapidity of the transition suggests that we are observing a genuine bifurcation rather than a qualitative change resulting from the slow depletion of the reactant concentrations in our closed system.

When the transition occurs relatively slowly, we can observe transitional patterns [Fig. 2(c)], short-lived SW with wavelength $\lambda_{SW}/2$ (the corresponding FFT possesses a broad spectrum of wavelengths from λ_{SW} to $\lambda_{SW}/2$) that quickly transform into TW of wavelength $\lambda_{SW}/2$. The TW contain several wave sources and sinks, as one would expect for TW originating from a wave instability [17], and several packets of waves can be seen propagating in different directions [see arrows in Fig. 2(d)]. The TW persist for tens of minutes.

The temporal oscillation periods of the SW before the transition and the TW after the transition measured at a

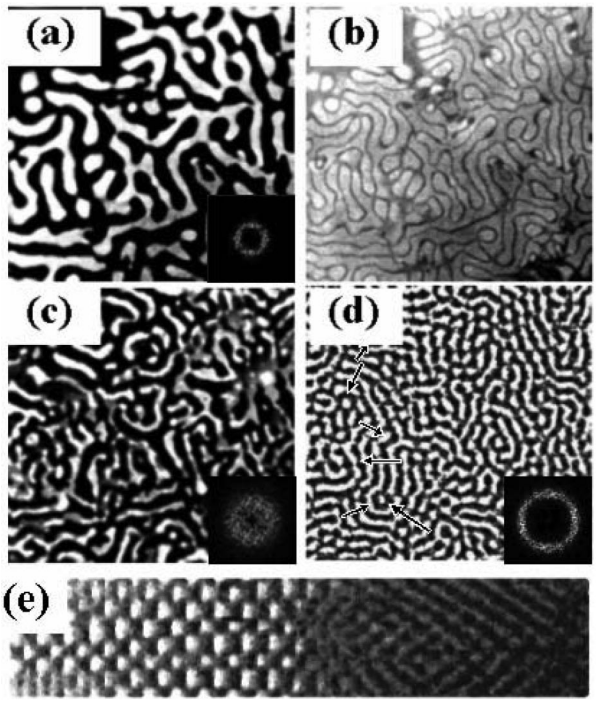

FIG. 2. Snapshots of (a) standing waves ($t = 1355$ s), (c) transitional patterns ($t = 1976$ s), and (d) traveling waves ($t = 2936$ s) found in the BZ-AOT/Span system. (b) A superposition of snapshot (a) and a snapshot taken half a period later; FFTs of snapshots (insets in bottom right corners) are used for calculating wavelengths in Fig. 3(a). Size = 3.05 mm × 2.92 mm. Concentrations as in Fig. 1(c), $\varphi_d = 0.66$. (e) Space-time plot (0.6 mm × 20 min, time increases from left to right) for SW-TW transition found at [MA] = 0.22 M, $[H_2SO_4] = 0.24$ M, all other parameters as above [conditions correspond to curve 1 in Fig. 3(a)]; for conditions of Figs. (a)–(d), the space-time plot is analogous to (e), but the SW(λ)-TW($\lambda/2$) transition is not as sharp.

single spatial point are identical, but the amplitude of the TW is approximately half that of the SW. The corresponding BZ-AOT/Span system in the STR has two regimes of oscillations: large amplitude, low frequency ($T =$ 60–90 s) and small amplitude, high frequency ($T =$ 20–30 s) [Fig. 3(b), curve 1]. We did not find any correlation between this transition in STR oscillations and the transition in patterns, though the period of the large amplitude oscillations is close to the period of the waves (1–1.3 min). SW patterns can coexist with high-frequency bulk oscillations for ca. 30 min, which suggests that our unstirred BZ-AOT/Span system possesses two different frequencies or two complex eigenvalues.

We found a strong correlation between the time, T_{tr}, at which the SW(λ)-TW($\lambda/2$) transition occurs, and the duration, T_{osc}, of oscillations in the STR. In Fig. 3(d), we see that $T_{tr} \approx cT_{osc} + \tau$, where the slope c is slightly less than 1. Simulations with an extended Oregonator model with additional variables $[Br_2]$ and $[BrO_2^{\bullet}]$ in the oil phase [8] augmented with slowly decreasing variable reactant concentrations [MA] and $[NaBrO_3]$ reveal that the rate of depletion of reactants differs for different dynamical regimes of the system. During STR (0D) oscillations, this rate is 10%–20% smaller than for 1D standing waves. If the SW(λ)-TW($\lambda/2$) transition is associated with the termination of bulk oscillations, we can therefore expect to find c in the range 0.8–1. We never observed the SW(λ)-TW($\lambda/2$) transition while the corresponding STR system still exhibited oscillations, though in some experiments we observed SW as well as the SW(λ)-TW($\lambda/2$) transition when no oscillations occurred in the STR [Fig. 3(b), curve 2] [18]. These observations suggest that the transition point lies close to and slightly below the Hopf bifurcation point.

In Fig. 3(c), we examine the system over a broad section of the ω_2-$[NaBrO_3]$ parameter plane. The region in which the wavelength-halving transition occurs is bordered by four zones: a steady state region in which no patterns occur; a region, which we did not study, in which the ME becomes cloudy; a region "λ" of SW with wavelength λ_{SW}; and a region "$\lambda/2$" with wavelength $\lambda_{TW} \cong \lambda_{SW}/2$ for both SW and TW patterns. Typical curves showing the time evolution of λ_{SW} and λ_{TW} are shown in Fig. 3(a) (curves 2 and 3), and the corresponding space-time plots appear in Figs. 3(f) and 3(e), respectively. In some experiments in the "$\lambda/2$" region, we observed the more familiar SW-TW transition at constant wavelength, as SW with wavelength $\lambda_{SW}/2$, analogous to the transient SW shown in Fig. 2(c), appeared first and then transformed into TW patterns. No bulk oscillations occur in the STR for compositions that belong to the "$\lambda/2$" region. The existence of the large regions "λ" and "$\lambda/2$" demonstrates that SW with wavelength λ and TW with wavelength $\lambda/2$ can exist independently for long times. The behavior described above in the "$\lambda/2$" region suggests that the SW(λ)-TW($\lambda/2$) transition may consist of two "elementary" transitions: SW(λ)-SW($\lambda/2$) and SW($\lambda/2$)-TW($\lambda/2$). We attribute the fact that in some cases we observe the SW-TW transition with the ratio $\lambda_{SW}/\lambda_{TW}$ less than 2 to the relatively long duration of these transitions and the proximity of the system to the boundary between the "$\lambda/2$" and "transition" [▲ in Fig. 3(c)] regions.

A single dynamical phenomenon, like antispirals [8,19] or labyrinthine stationary patterns [7,20], can arise via quite different mechanisms. We consider here two interpretations of the SW(λ)-TW($\lambda/2$) transition we have observed.

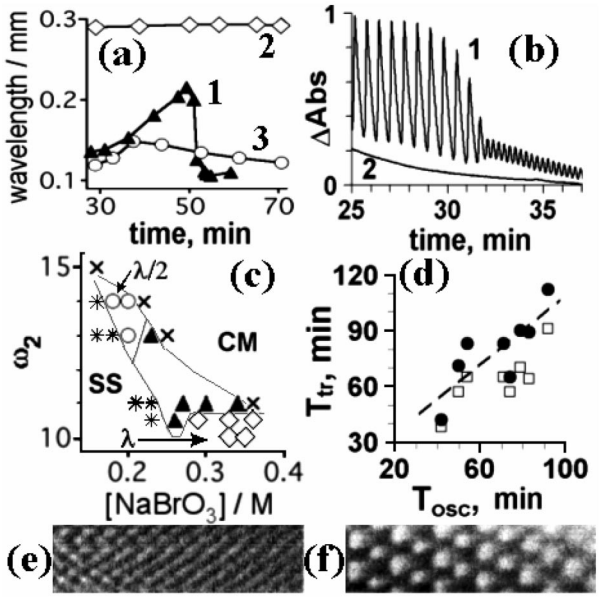

FIG. 3. (a) Typical variation of wavelength with time for three regions shown in (c): (curve 1) region of SW(λ)-TW($\lambda/2$) transition at $\omega_2 = 11$, $[NaBrO_3] = 0.3$ M; (curve 2) region "λ" at $\omega_2 = 10.5$, $[NaBrO_3] = 0.36$ M; (curve 3) region "$\lambda/2$" at $\omega_2 = 14$, $[NaBrO_3] = 0.18$ M; other conditions are $\varphi_d = 0.66$, $\rho = 0.429$, [MA] = 0.22 M, $[H_2SO_4] = 0.24$ M, and [bathoferroin] = 4 mM. (b) Bulk behaviors in the STR for concentrations corresponding to the SW(λ)-TW($\lambda/2$) transition in spatially extended system at $\rho = 0.429$, $\varphi_d = 0.65$, $[NaBrO_3] = 0.27$ M, [MA] = 0.22 M, $[H_2SO_4] = 0.25$ M, and [bathoferroin] = 4 mM, and $\omega_2 =$ (curve 1) 10.5, (curve 2) 10. $\Delta Abs = 1$ is equivalent to Δ[bathoferroin] = 3.6 mM. (c) Dynamical behavior in the $[NaBrO_3]$-ω_2 plane. Symbols: (○, "$\lambda/2$" region) SW-TW transition without wavelength change, (◇, "λ" region) SW without transition, (▲) SW-TW transition accompanied by wavelength halving, (*) homogeneous steady state, (×) cloudy ME. (d) Time of cessation of bulk oscillations (T_{osc}) and time of SW(λ)-TW($\lambda/2$) transition, T_{tr}, shown as the beginning of the transition (□) and the beginning of clearly seen traveling waves (●); trend line $T_{tr} = 0.94T_{osc} + 15.1$, $\omega_2 = 10.5$–11, $\rho = 0.429$, $\varphi_d = 0.66$, $[NaBrO_3] =$ 0.27–0.3 M, [MA] = 0.22 M, $[H_2SO_4] =$ 0.22–0.25 M, and [bathoferroin] = 4 mM. (e),(f) Time-space plots (0.6 mm × 20 min) corresponding to curves 3 and 2, respectively, in (a). Low contrast in right part of (f) reflects the fact that SW in region "λ" smoothly fade out.

First, interaction between wave, Hopf, and possibly Turing instabilities may result in a SW-TW transition with wavelength halving (subharmonic wavelength) analogous to the Turing-Hopf interaction that leads to antiphase oscillatory Turing patterns [21] or to the wavelength doubling cascade in 3D nematic liquid crystals [22,23]. However, no theory of such a phenomenon is available at present. Our simulations with an extended Oregonator model and experimental data reveal that the system behavior is very sensitive to the ratio $a = [NaBrO_3]/[MA]$, if a is close to 1–1.5. During the course of the reaction, a changes, as well as the concentrations of the most important intermediates like $[Br_2]$, [BrMA] (bromomalonic acid), and $[BrO_2^{\bullet}]$, which first increase with time and then decrease.

An alternative interpretation involves the mechanism of synchronization among the nanodroplets or nano-oscillators. Mass exchange between large droplets (0.1 μm in diameter) should be able to produce synchronization over short distances (1 μm). Dynamical water channels between droplets can extend this distance to ca. 10 μm. Fast-diffusing Br_2 (and/or $BrO_2^{\bullet}$) in the oil phase can contribute to synchronization at even longer distances (100 μm). An increase in $[Br_2]$ as the reaction proceeds, for example, might switch the regime of synchronization of the nano-oscillators [like those shown in Fig. 3(b), curve 1], while a decrease in $[Br_2]$ might terminate bulk oscillations in 0D.

Usually, problems involving synchronization of many oscillators are studied only in 0D [24]. Coupling of the period of oscillation T_0 with the diffusion coefficient D of the communicating entities in 1D or 2D by the diffusion relation $DT_0 \cong \lambda^2$ yields a characteristic wavelength λ. With $\lambda = \lambda_{SW} = 0.22$–$0.28$ mm, $D = 10^{-5}$ cm^2/s, and $T_0 = 60$–90 s (the period of oscillations of SW and TW), this relation holds true. Our system possesses a second, shorter period for the bulk oscillations ($T_b = 20$–30 s), which can potentially give rise to a shorter characteristic wavelength, λ_2. In this ''synchronization'' scenario, transition from one regime of behavior (frequencies in a STR or patterns in a layer) to another can occur only if different spatial (λ, λ_2) or temporal (T_0, T_b) modes (or their subharmonics) can interact strongly, for example, when $\lambda{:}\lambda_2 = 2$. This hypothesis suggests a situation in which a single nanoreactor can support oscillations, while there are no macro-oscillations in the STR, owing to a lack of global synchronization [as in curve 2 in Fig. 3(b)] even with intensive stirring because of the high viscosity of the microemulsion. As in the case of our first interpretation, no clear theory of such a phenomenon is available at present.

We have described a new SW(λ)-TW($\lambda/2$) transition found in a microheterogeneous system that consists of a very large number (ca. 10^{10} in a volume $\lambda^2 h$ and 10^{14} in the entire reactor) of coupled chemical nano-oscillators. Understanding the patterns and bifurcations that arise in this very complex, but tunable and well-characterized, system should be a useful step toward elucidating the behavior of systems like bacterial colonies or living tissues that are also composed of myriad interacting subunits.

This work was supported by Grant No. CHE-0306262 from the Chemistry Division of the National Science Foundation.

[1] P. Kolodner, Phys. Rev. E **48**, R665 (1993).
[2] D. P. Vallette, W. S. Edwards, and J. P. Gollub, Phys. Rev. E **49**, R4783 (1994).
[3] O. Lev, M. Sheintuch, L. M. Pisemen, and Ch. Yarnitzky, Nature (London) **336**, 458 (1988).
[4] M. Bertram, C. Beta, M. Pollmann, A. S. Mikhailov, H. H. Rotermund, and G. Ertl, Phys. Rev. E **67**, 036208 (2003).
[5] S. Jakubith, H. H. Rotermund, W. Engel, A. von Oertzen, and G. Ertl, Phys. Rev. Lett. **65**, 3013 (1990).
[6] A. Magnani *et al.*, J. Am. Chem. Soc. **126**, 11 406 (2004).
[7] V. K. Vanag and I. R. Epstein, Phys. Rev. Lett. **87**, 228301 (2001).
[8] V. K. Vanag and I. R. Epstein, Phys. Rev. Lett. **88**, 088303 (2002).
[9] V. K. Vanag and I. R. Epstein, J. Chem. Phys. **121**, 890 (2004).
[10] M. C. Cross and P. C. Hohenberg, Rev. Mod. Phys. **65**, 851 (1993).
[11] H. Sakaguchi, Phys. Scr. **T67**, 148 (1996).
[12] M. Dolnik, A. M. Zhabotinsky, A. B. Rovinsky, and I. R. Epstein, Chem. Eng. Sci. **55**, 223 (2000).
[13] A. M. Zhabotinsky, M. Dolnik, and I. R. Epstein, J. Chem. Phys. **103**, 10 306 (1995).
[14] M. J. Hou and D. O. Shah, Langmuir **3**, 1086 (1987).
[15] V. K. Vanag and I. R. Epstein, Proc. Natl. Acad. Sci. U.S.A. **100**, 14 635 (2003).
[16] See EPAPS Document No. E-PRLTAO-95-075532 for movies of this transition. This document can be reached via a direct link in the online article's HTML reference section or via the EPAPS homepage (http://www.aip.org/pubservs/epaps.html).
[17] M. van Hecke, C. Storm, and W. van Saarloos, Physica (Amsterdam) **134D**, 1 (1999).
[18] Although the absence of oscillations in the STR usually occurs for ME that are close to the SS region shown in Fig. 3(c), there are no evident regularities in emergence (or absence) of bulk oscillations in the STR for those compositions at which the SW(λ)-TW($\lambda/2$) transition is observed.
[19] Y. Gong and D. J. Christini, Phys. Rev. Lett. **90**, 088302 (2003).
[20] K. J. Lee, W. D. McCormick, Q. Ouyang, and H. L. Swinney, Science **261**, 192 (1993).
[21] A. De Wit, D. Lima, G. Dewel, and P. Borckmans, Phys. Rev. E **54**, 261 (1996).
[22] A. G. Rossberg, N. Eber, A. Buka, and L. Kramer, Phys. Rev. E **61**, R25 (2000).
[23] C. Fradin, P. L. Finn, H. R. Brand, and P. E. Cladis, Phys. Rev. Lett. **81**, 2902 (1998).
[24] S. H. Strogatz, *Nonlinear Dynamics and Chaos. With Applications to Physics, Biology, Chemistry, and Engineering* (Addison-Wesley, Reading, MA, 1994).